

## Comparison of the Dehalogenation of Dihalomethanes (CH<sub>2</sub>XI, where X = Cl, Br, I) Following Ultraviolet Photolysis in Aqueous and NaCl Saltwater Environments

Yong Du, Xiangguo Guan, Wai Ming Kwok, Lai Man Chu, and David Lee Phillips\*

Department of Chemistry, The University of Hong Kong, Pokfulam Road, Hong Kong S.A.R., P.R. China

Received: January 28, 2005; In Final Form: May 10, 2005

The ultraviolet photolysis of low concentrations of CH<sub>2</sub>XI (X = Cl, Br, I) were investigated in water and saltwater solutions by photochemistry and picosecond time-resolved resonance Raman spectroscopy. Photolysis in both kinds of solutions formed mostly CH<sub>2</sub>(OH)<sub>2</sub> and HI and HX products. However, photolysis of the CH<sub>2</sub>XI molecules in saltwater resulted in production of some CH<sub>2</sub>XCl products not observed in aqueous solutions without salt present. The appearance of these new products in saltwater solutions is accompanied by a decrease in the amount of CH<sub>2</sub>(OH)<sub>2</sub>, HI, and HX products compared to photolysis in aqueous solutions without salt present. The possible implications for photolysis of CH<sub>2</sub>XI and other polyhalomethanes in seawater and other salt aqueous environments compared to nonsaltwater solvated environments is briefly discussed.

### Introduction

A range of polyhalomethanes such as CH<sub>2</sub>I<sub>2</sub>, CH<sub>2</sub>BrI, CH<sub>2</sub>-CII, CHBr<sub>3</sub>, CCl<sub>4</sub>, CFCI<sub>3</sub>, and others, have been observed in the natural environment and are significant sources of reactive halogens.<sup>1–8</sup> The photochemistry of CH<sub>2</sub>I<sub>2</sub> and CH<sub>2</sub>BrI has been linked to the production of IO during localized ozone depletion in the marine boundary layer of the troposphere.<sup>7,8</sup> The photochemistry of CH<sub>2</sub>I<sub>2</sub> has also been linked to the formation of iodine aerosols in the marine boundary layer.<sup>9</sup> It is useful to understand both gas and condensed phase chemistry and photochemistry to accurately describe many chemical reaction processes in the natural environment.<sup>9–21</sup> The chemical reactions relevant to the activation of halogens in aqueous sea-salt particles have been a topic receiving significant interest.<sup>10–21</sup>

Ultraviolet photolysis of gas phase polyhalomethanes typically results in a direct carbon–halogen bond cleavage to produce halomethyl radical and halogen atom fragments.<sup>22–38</sup> In the condensed phase, these fragments can undergo solvent-induced geminate recombination to produce noticeable amounts of isopolyhalomethanes that have some ion-pair character.<sup>39–55</sup> Ultraviolet photolysis of polyhalomethanes in condensed phase environments has also been reported to produce radical and ionic fragments.<sup>56–62</sup> Some studies suggested that carbon–halogen bonds in polar media have an electron transfer between the two radical fragments within the solvent cage to produce ionic species in some halocarbons.<sup>61,62</sup> We have investigated experimentally and theoretically the chemical reactivity of isopolyhalomethanes toward C=C bonds in olefins and discovered that isopolyhalomethane carbenoids are able to react with the C=C bonds to produce cyclopropanated products and a halogen molecule leaving group.<sup>63–69</sup> The studies on isodiiodomethane (CH<sub>2</sub>I–I) indicated that it is the carbenoid species mainly responsible for the cyclopropanation of olefins when employing the ultraviolet photolysis of CH<sub>2</sub>I<sub>2</sub> method.<sup>63,65,68</sup> This led to a reaction mechanism being proposed for the cyclopropanation of olefins by using ultraviolet photolysis of polyhalo-

methanes.<sup>63–65,67–69</sup> Another group has recently investigated solvent effects on the reactions of isodiiodomethane with olefins.<sup>70</sup>

Carbenoids and carbenes can also react with the O–H bonds of water and alcohols via an O–H insertion process.<sup>71–80</sup> We employed picosecond time-resolved resonance Raman (ps-TR<sup>3</sup>) experiments to directly observe the O–H insertion reaction of the isobromoform species with water to produce a CHBr<sub>2</sub>OH product and this indicates isopolyhalomethanes may also react with the O–H bonds of water via O–H insertion similar to other carbenoids and carbenes.<sup>81,82</sup> We have recently examined the photochemistry of low concentrations of dihalomethanes (CH<sub>2</sub>XI where X = Cl, Br, I) in water and water/acetonitrile mixed solvents and observed the dihalomethanes were mostly converted into CH<sub>2</sub>(OH)<sub>2</sub> plus HX and HI products.<sup>83,84</sup> Ps-TR<sup>3</sup> experiments observed noticeable amounts of isodihalomethanes (CH<sub>2</sub>X–I where X = Cl, Br, I) were made within several picoseconds and then decayed more quickly as the water concentration increased in mixed water/acetonitrile solvents suggesting the isodihalomethanes may be reacting with water.<sup>83,84</sup> Ab initio computations indicated the CH<sub>2</sub>X–I (X = Cl, Br, I) species could react with water via water-catalyzed O–H insertion/HI elimination reactions followed by their CH<sub>2</sub>X(OH) halomethanol product further decomposing by a water-catalyzed HX elimination reaction to produce a formaldehyde (CH<sub>2</sub>CO) that then react with water to produce the methanediol (CH<sub>2</sub>(OH)<sub>2</sub>) product observed in the photochemistry experiments.<sup>83,84</sup> Photolysis of low concentrations of CH<sub>2</sub>I<sub>2</sub> in saltwater was also found to produce mainly the CH<sub>2</sub>(OH)<sub>2</sub> and 2HI products observed in pure water.<sup>83–85</sup> However, new products/intermediates (CH<sub>2</sub>CII and Cl<sub>2</sub><sup>–</sup>) were observed in the saltwater solvent that were not observed in the absence of salt indicating the photochemistry of polyhalomethanes can be somewhat different in saltwater than in water.<sup>83–85</sup>

In this paper, we investigate the photochemistry of a series of dihalomethanes (CH<sub>2</sub>I<sub>2</sub>, CH<sub>2</sub>BrI, and CH<sub>2</sub>CII) in saltwater environments and compare these results to those recently obtained in aqueous environments where salt is absent.<sup>83,84</sup> All three of these dihalomethanes have been observed in the marine boundary layer.<sup>7</sup> Photochemistry experiments observed that

\* To whom correspondence should be addressed. Phone: 852-2859-2160. Fax: 852-2857-1586. E-mail: phillips@hkucc.hku.hk.

ultraviolet photolysis of low concentrations of all three molecules in saltwater still led to mainly formation of  $\text{CH}_2(\text{OH})_2$  and HX and HI products similar to photolysis in aqueous solvents with no salt present. However, new  $\text{CH}_2\text{XCl}$  (where  $\text{X} = \text{Cl}, \text{Br}, \text{I}$ ) products were produced in noticeable amounts in the saltwater solvents while these products did not appear in the water solvents without salt present. We compare how adding salt to the aqueous solvent affects the photochemistry of the  $\text{CH}_2\text{XI}$  ( $\text{X} = \text{Cl}, \text{Br}, \text{I}$ ) dihalomethanes and also very briefly discuss the potential influence of this photochemistry on the decomposition of polyhalomethanes in aqueous environments with and without salt present.

## Experimental Methods

**Photochemistry Experiments.** Commercially available  $\text{CH}_2\text{I}_2$  (99%),  $\text{CH}_2\text{BrI}$  (98%),  $\text{CH}_2\text{ClI}$  (>97%),  $\text{D}_2\text{O}$  (99.9% D), deionized water, and NaCl were used to prepare samples of about  $1 \times 10^{-4}$  M  $\text{CH}_2\text{XI}$  (where  $\text{X} = \text{Cl}, \text{Br}, \text{I}$ ) in water and 0.5 M NaCl aqueous solutions for use in the photochemistry experiments. The stated purity of the commercial dihalomethanes was consistent with the  $^1\text{H}$  NMR spectra of them. A micropipet was used to introduce the dihalomethanes into the deionized water solvent. These sample solutions were placed in an airtight glass holder having quartz windows with a 10 cm path length. The samples were shaken by hand for 0.5 h and allowed to stand for 1 day in the dark. There was no trace of any undissolved dihalomethane in the samples and no precipitate was observed. The UV-vis spectra of the  $\text{CH}_2\text{I}_2$  samples were found to obey Beer's law over the 0 to  $1.75 \times 10^{-4}$  M concentration range (see Figure S1 in the Supporting Information) and there was no evidence of significant amounts of aggregates at the concentrations used in the photochemistry experiments. The maximum molar extinction coefficient for  $\text{CH}_2\text{I}_2$  in water was found to be about  $1190 \text{ cm}^{-1} \text{ M}^{-1}$  at about 270 nm. The molar extinction coefficients for  $\text{CH}_2\text{I}_2$ ,  $\text{CH}_2\text{BrI}$ , and  $\text{CH}_2\text{ClI}$  at 266 nm in pure water were found to be 1185, 985, and  $458 \text{ cm}^{-1} \text{ M}^{-1}$ , respectively, and in saltwater to be 971, 584, and  $413 \text{ cm}^{-1} \text{ M}^{-1}$ , respectively. An unfocused 266 nm laser beam (about 3 mJ per pulse) from the fourth harmonic of a Nd:YAG laser was used to excite the samples in the photochemistry experiments. Some additional samples that were housed in an airtight quartz tube were also irradiated by natural sunlight as described later in the discussion section. The absorption spectra for the photolyzed samples were obtained using an airtight 1 cm UV grade cell and a Perkin-Elmer Lambda 18 UV/VIS spectrometer and the pH was measured with use of a 8102BN combination electrode that was calibrated with 7.00 pH and 4.01 pH buffer solutions.  $^1\text{H}$  NMR spectra were obtained with a Bruker Advance 400 DPX spectrometer and  $\phi = 5$  mm sample tubes at room temperature. The UV-vis spectrometer was calibrated over the 210 to 250 nm region with standard samples of NaI dissolved in water (see Figure S2 in the Supporting Information). The UV-vis spectra of the  $\text{I}^-$  ion was observed to obey Beer's law over the  $5 \times 10^{-6}$  to  $10^{-4}$  M range and the  $\text{I}^-$  spectrum was observed to be identical with that seen after photolysis of the iodine containing dihalomethanes in water and saltwater samples.

**Picosecond Time-Resolved Resonance Raman (Ps-TR<sup>3</sup>) Experiments.** The experimental apparatus and methods have been detailed elsewhere<sup>81–85</sup> so only a short description is given here. The output (800 nm, 1 ps, 1 kH) from a commercial femtosecond mode-locked Ti:Sapphire regenerative amplifier laser was doubled and tripled by using KDP crystals to make the 400 nm probe and 267 nm pump excitation wavelengths

used in the experiments. Fluorescence depletion of *trans*-stilbene was used to find the time-zero delay between the pump and probe laser beams as described in previous work<sup>81–85</sup> and estimated to be accurate to  $\pm 0.5$  ps with a typical cross-correlation time of about 1.5 ps full width half-maximum. A magic angle polarization was used to loosely focus the pump and probe laser beams onto a flowing liquid stream of sample (about 500  $\mu\text{m}$  thick). Typical pulse energies and spot sizes were 15  $\mu\text{J}$  and 250  $\mu\text{m}$  for the pump beam and 8  $\mu\text{J}$  and 150  $\mu\text{m}$  for the probe beam. The sample was excited with a backscattering geometry and reflective optics were employed to collect the Raman scattered light that was then imaged through the entrance slit of the spectrograph whose grating dispersed the Raman light onto a liquid nitrogen cooled CCD detector.

Each spectrum shown was found by subtraction of scaled probe-before-pump and scaled net solvent measurements from a pump-probe spectrum so as to remove the ground-state  $\text{CH}_2\text{XI}$  Raman bands and residual solvent Raman bands, respectively. The spectra were calibrated with an estimated uncertainty of  $\pm 5 \text{ cm}^{-1}$  in absolute frequency by using the known Raman shifts of the solvent Raman bands. Sample solutions of  $\text{CH}_2\text{XI}$  ( $\text{X} = \text{Cl}, \text{Br}, \text{I}$ ) of about  $7 \times 10^{-3}$  M with varying salt concentrations (0.0, 0.2, and 0.5 M NaCl) were prepared in a 75% water/25% acetonitrile by volume solvent for use in the ps-TR<sup>3</sup> experiments. The samples exhibited less than a few percent decomposition during the experiments as deduced from UV-vis spectra obtained before and after the ps-TR<sup>3</sup> experiments.

## Results and Discussion

**Photochemistry Experiments.** Figure 1 presents ultraviolet/visible spectra obtained following varying times of 266 nm laser photolysis for  $\text{CH}_2\text{I}_2$ ,  $\text{CH}_2\text{BrI}$ , and  $\text{CH}_2\text{ClI}$  in pure water and in saltwater (0.5 M NaCl) solutions. Inspection of Figure 1 shows that in both cases the absorption bands due to the parent  $\text{CH}_2\text{XI}$  ( $\text{X} = \text{Cl}, \text{Br}, \text{I}$ ) in the 250–320 nm region decrease in intensity while those due to the  $\text{I}^-$  ion in the 225 nm region increase in intensity as the photolysis time increases. In the case of the  $\text{CH}_2\text{BrI}$  molecule, the increase in the  $\text{I}^-$  absorption band is accompanied by a simultaneous increase in the  $\text{Br}^-$  absorption band around 195 nm in the pure water solution. Examination of Figure 1 shows clear isobestic points around 253 nm between the  $\text{I}^-$  absorption band and the parent  $\text{CH}_2\text{XI}$  ( $\text{X} = \text{Cl}, \text{Br}, \text{I}$ ) and indicate the  $\text{I}^-$  is produced directly from the parent  $\text{CH}_2\text{XI}$  molecule. The pH of the sample solutions was also determined when each of the absorption spectra was acquired during the photolysis experiments. The molar extinction coefficients for the  $\text{CH}_2\text{XI}$  ( $\text{X} = \text{Cl}, \text{Br}, \text{I}$ ) molecules and the  $\text{I}^-$  ion were utilized to obtain the concentrations of these species from the absorption spectra in Figure 1 for each of the photolysis times. These concentrations were then used to determine the changes in the concentrations of these species ( $-\Delta[\text{CH}_2\text{XI}]$  and  $[\text{I}^-]$ ) as a function of photolysis time. Figure 2 displays plots of  $-\Delta[\text{CH}_2\text{XI}]$  versus  $[\text{I}^-]$  for photolysis of  $\text{CH}_2\text{XI}$  ( $\text{X} = \text{Cl}, \text{Br}, \text{I}$ ) in water and saltwater (0.5 M NaCl) solutions obtained from analysis of the spectra in Figure 1. The increase in  $[\text{I}^-]$  versus the decrease in  $[\text{CH}_2\text{XI}]$  during the photolysis experiments (see Figure 2) exhibit linear relationships with slopes of about 2 for  $\text{X} = \text{I}$  and about 1 for  $\text{X} = \text{Br}, \text{Cl}$  in water solvent, and about 1.4 for  $\text{X} = \text{I}$ , 0.9 for  $\text{X} = \text{Br}$ , and 0.6 for  $\text{X} = \text{Cl}$  in saltwater (0.5 M NaCl) solutions. The ultraviolet photolysis of  $\text{CH}_2\text{XI}$  ( $\text{X} = \text{Cl}, \text{Br}, \text{I}$ ) at low concentrations in saltwater solvent appears to release fewer  $\text{I}^-$  ions per  $\text{CH}_2\text{XI}$  molecule compared to

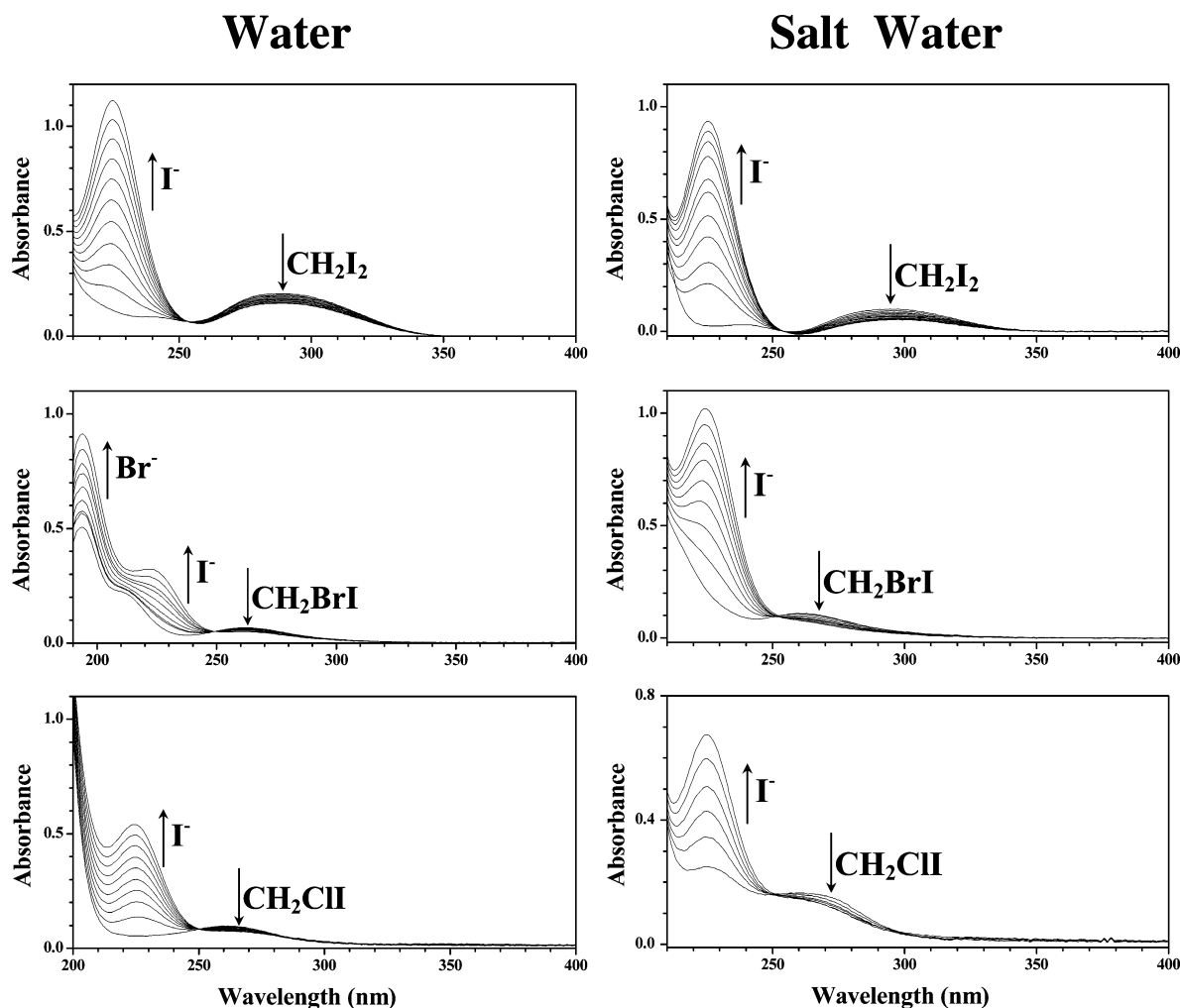
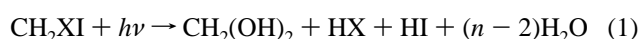


**Figure 1.** Ultraviolet/visible spectra obtained following varying times of 266 nm laser photolysis of about  $1 \times 10^{-4}$  M CH<sub>2</sub>I<sub>2</sub>, CH<sub>2</sub>BrI, and CH<sub>2</sub>ClI in pure water (left column) and in 0.5 M NaCl saltwater (right column) solutions. The parent dihalomethane absorption bands decrease with increasing photolysis time and new absorption bands due to I<sup>-</sup> appear at about 225 nm. In the case of CH<sub>2</sub>BrI a new absorption band due to Br<sup>-</sup> appears at about 197 nm.

photolysis in water solvent. For example, the slopes of  $-\Delta[\text{CH}_2\text{XI}]$  versus  $[\text{I}^-]$  as a function of photolysis time in Figure 2 indicate about 2 I<sup>-</sup> are formed in water solvent versus 1.4 I<sup>-</sup> in saltwater solvent for photolysis of CH<sub>2</sub>I<sub>2</sub>. Figure 3 presents plots of the changes observed in the [H<sup>+</sup>] concentrations obtained from the pH measurements versus the changes in the [I<sup>-</sup>] concentrations as a function of photolysis times for CH<sub>2</sub>XI (X = Cl, Br, I) in water and saltwater solvents. The plots of  $\Delta[\text{H}^+]$  versus  $\Delta[\text{I}^-]$  have linear correlation and slopes of about 1.1 for X = I and 2.2 for X = Br and Cl in pure water solvent and slopes of about 0.8 for X = I, 1.6 for X = Br, and 1.3 for X = Cl in saltwater solvent. These results suggest that in the pure water solvents one H<sup>+</sup> is formed for each I<sup>-</sup> produced from CH<sub>2</sub>I<sub>2</sub> while two H<sup>+</sup> are formed for each I<sup>-</sup> produced from CH<sub>2</sub>BrI and CH<sub>2</sub>ClI. In our previous work in pure water solutions, we found that [Br<sup>-</sup>] was produced from photolysis of [CH<sub>2</sub>BrI] and plots of  $\Delta[\text{Br}^-]$  versus  $-\Delta[\text{CH}_2\text{BrI}]$  and  $\Delta[\text{H}^+]$  versus  $\Delta[\text{Br}^-]$  had linear relationships with slopes of about  $0.9 \pm 0.1$  and  $2.2 \pm 0.2$ , respectively. These results show one Br<sup>-</sup> ion is released after photolysis of CH<sub>2</sub>BrI in water, and when this is combined with the changes in the pH and I<sup>-</sup> and CH<sub>2</sub>BrI concentrations it indicates that photolysis of low concentrations of CH<sub>2</sub>BrI in water leads to 2H<sup>+</sup>, Br<sup>-</sup>, and I<sup>-</sup> products. These products are likely produced from HI and HBr leaving groups that dissociate into H<sup>+</sup> and I<sup>-</sup> and H<sup>+</sup> and Br<sup>-</sup>, respectively, in water.

To learn more about what happens to the carbon atom after photolysis of the CH<sub>2</sub>XI molecules at low concentrations in water and saltwater solutions, we have done the same ultraviolet photolysis experiments and used <sup>1</sup>H NMR to examine the products produced. Figure 4 presents the <sup>1</sup>H NMR spectra obtained before and after photolysis of CH<sub>2</sub>XI (X = Cl, Br, I) in D<sub>2</sub>O and 0.5 M NaCl D<sub>2</sub>O solutions. In all of the cases shown in Figure 4 the photolysis of the parent compound converts it into mostly methanediol (CH<sub>2</sub>(OD)<sub>2</sub>) product. However, in the saltwater solutions, new <sup>1</sup>H NMR bands appear after photolysis and these are assigned to CH<sub>2</sub>XCl (X = Cl, Br, I), which was confirmed by comparison to spectra of authentic samples. The results in Figure 4 are in agreement with previous <sup>1</sup>H and <sup>13</sup>C NMR experiments done for ultraviolet photolysis of low concentrations of CH<sub>2</sub>I<sub>2</sub> and <sup>13</sup>CH<sub>2</sub>I<sub>2</sub> in water and saltwater solutions.<sup>83,85</sup>

The preceding photochemistry results in conjunction with previous results obtained in pure water solutions<sup>83,84</sup> suggest the major reaction occurring after ultraviolet photolysis of low concentrations of CH<sub>2</sub>XI (X = Cl, Br, I) in water and saltwater solutions is the following reaction:



We note that in saltwater this is not the only significant reaction and formation of the CH<sub>2</sub>XCl (X = Cl, Br, I) product also takes

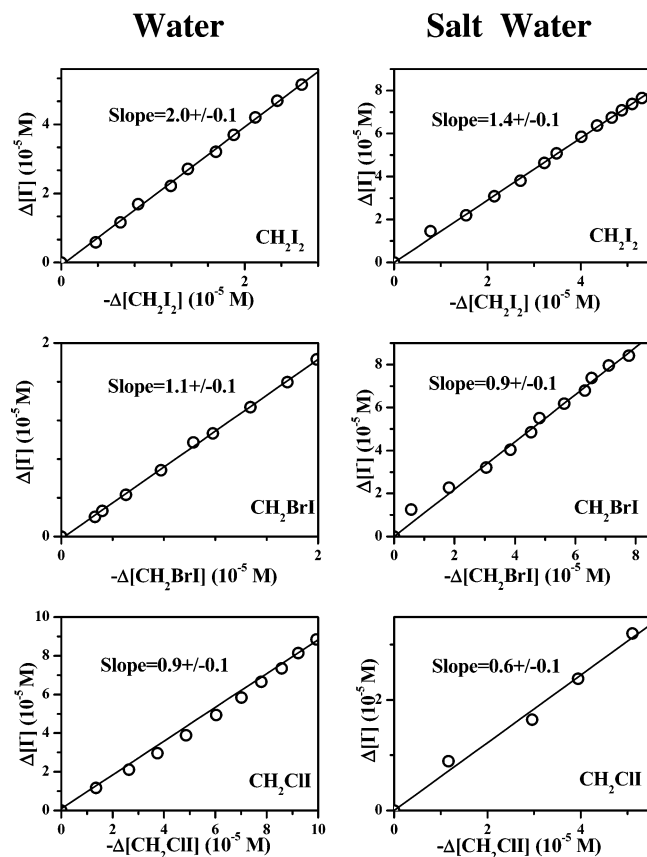


**Figure 2.** Plots of  $-\Delta[\text{CH}_2\text{XI}]$  versus  $[\text{I}^-]$  for photolysis of  $\text{CH}_2\text{XI}$  ( $X = \text{Cl}, \text{Br}, \text{I}$ ) in water (left column) and 0.5 M NaCl saltwater (right column) solutions obtained from analysis of the spectra shown in Figure 1. The increase in  $[\text{I}^-]$  versus the decrease in  $[\text{CH}_2\text{XI}]$  during the photolysis experiments exhibits a linear relationship with slopes indicated above the linear least-squares best fit (solid line in the plots of the data).

place and this indicates another competing reaction occurs in saltwater environments. Previous experiments done for  $\text{CH}_2\text{I}_2$  with use of a Hg lamp source of light led to essentially the same results as found for the unfocused nanosecond laser photolysis experiments (see ref 76) and this suggests that the photoproducts observed in Figures 1 and 4 are produced from mostly one-photon excitation. To better understand the intermediates involved in the chemistry leading to the final products seen in the photochemistry experiments, further picosecond time-resolved resonance Raman (ps-TR<sup>3</sup>) spectroscopy experiments were done and these are given in the next section.

**Picosecond Time-Resolved Resonance Raman (Ps-TR<sup>3</sup>) Experiments.** Figure 5 displays ps-TR<sup>3</sup> acquired after 267 nm photolysis of  $\text{CH}_2\text{XI}$  ( $X = \text{Cl}, \text{Br}, \text{I}$ ) in 0.0 M NaCl, 0.2 M NaCl, and 0.5 M NaCl 75%  $\text{H}_2\text{O}/25\%$   $\text{CH}_3\text{CN}$  solvents. The ps-TR<sup>3</sup> spectra in Figure 5 are similar to those previously observed after 267 nm photolysis of  $\text{CH}_2\text{I}_2$ ,  $\text{CH}_2\text{BrI}$ , and  $\text{CH}_2\text{ClI}$  in largely aqueous solutions.<sup>84</sup> The vibrational assignments for the intermediates generated within several picoseconds and decaying on the tens to hundreds of picoseconds time scale are straightforward to assign to isodihalomethanes that have been previously studied with time-resolved resonance Raman spectroscopy.<sup>46,47,49,52,53,55,65</sup> References 47, 55, and 65 provide details of the assignments of the isodiiodomethane ( $\text{CH}_2\text{I}-\text{I}$ ) intermediate produced after ultraviolet photolysis of  $\text{CH}_2\text{I}_2$  in liquid solutions. For the isobromomethane ( $\text{CH}_2\text{Br}-\text{I}$ ) intermediate formed after photolysis of  $\text{CH}_2\text{BrI}$ , refs 46, 49, and 53 provide details of the vibrational assignments. Reference 52 provides

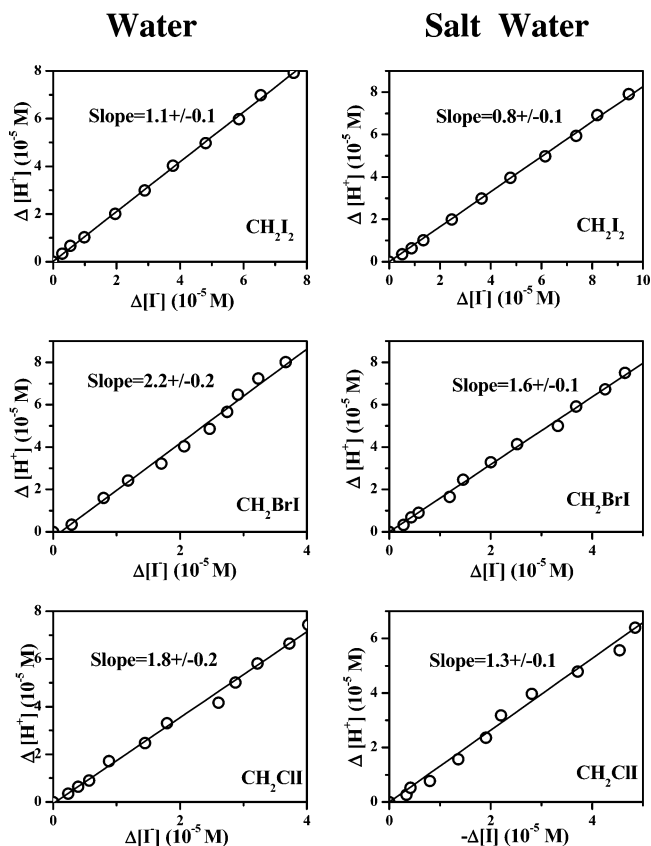


**Figure 3.** Plots of the changes observed in the  $[\text{H}^+]$  concentrations obtained from the pH measurements versus the changes in the  $[\text{I}^-]$  concentrations as a function of photolysis times for  $\text{CH}_2\text{XI}$  ( $X = \text{Cl}, \text{Br}, \text{I}$ ) in water (left column) and saltwater (right column) solvents. The plots of  $\Delta[\text{H}^+]$  versus  $\Delta[\text{I}^-]$  have a linear correlation with slopes indicated above the linear least-squares best fit (solid line in the plots of the data).

details of the vibrational assignments of the isochloroiodomethane ( $\text{CH}_2\text{Cl}-\text{I}$ ) species formed after ultraviolet photolysis of  $\text{CH}_2\text{ClI}$  in liquids. For the convenience of readers of this paper, we have included Tables S1–S3 (in the Supporting Information) giving the vibrational assignments for the present isopolyhalomethane spectra. Tables S1–S3 also compare these assignments with previous vibrational assignments from the preceding references as well as with previously predicted vibrational frequencies for the relevant isodihalomethanes and several other species that have been proposed to be formed after photolysis of dihalomethanes in condensed phase environments.

Using the spectra of isodiiodomethane as an example, we will briefly go over how the TR<sup>3</sup> spectra were assigned to the isodihalomethane species. Figure S3 in the Supporting Information presents the TR<sup>3</sup> spectrum obtained after ultraviolet photolysis of  $\text{CH}_2\text{I}_2$  in cyclohexane solvent, using a nanosecond pulsed laser. This spectrum is compared in Figure S3 to TR<sup>3</sup> spectra obtained in cyclohexane solvent at 500 ps, in acetonitrile solvent at 100 ps, using a picosecond laser (from ref 50) and in a 0.5 M NaCl 75% water/25% acetonitrile solution, using a picosecond laser (this work). Examination of Figure S3 reveals that all of the spectra are very similar to one another with intense resonance Raman bands that can be assigned to the fundamentals, overtones, and combination bands of several Franck–Condon active vibrational modes. The most intense Raman bands are a low-frequency mode in the 118–128  $\text{cm}^{-1}$  region that has a significant overtone progression and combination bands with a strong fundamental in the 700–720  $\text{cm}^{-1}$  region

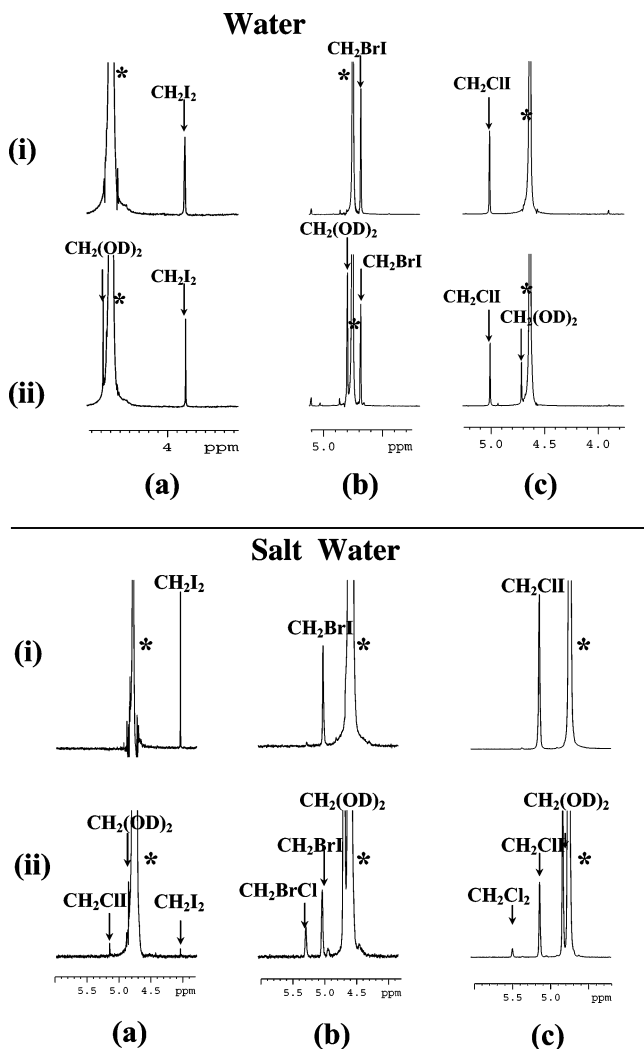


**Figure 4.**  $^1\text{H}$  NMR spectra obtained before (i) and after appreciable (ii) 266 nm photolysis of  $\text{CH}_2\text{I}_2$  (a),  $\text{CH}_2\text{BrI}$  (b), and  $\text{CH}_2\text{ClI}$  (c) in  $\text{D}_2\text{O}$  and 0.5 M NaCl  $\text{D}_2\text{O}$  solutions. In all the cases photolysis converts the dihalomethane mostly into a methanediol product ( $\text{CH}_2(\text{OD})_2$ ). However, in the saltwater solutions new bands due to  $\text{CH}_2\text{XCl}$  (X = Cl, Br, I) are also observed after photolysis. See the text for more details.

and a moderate intensity fundamental near  $620\text{ cm}^{-1}$ . Table S1 presents the predicted vibrational modes for species that have been proposed to be formed after photolysis of  $\text{CH}_2\text{I}_2$  in condensed phase environments:  $\text{CH}_2\text{I}-\text{I}$  (isodiiodomethane),  $\text{CH}_2\text{I}_2^+$  cation,  $\text{CH}_2\text{I}$  radical, and the  $\text{CHI}$  carbene. One would expect the fundamentals of the totally symmetric Franck-Condon active modes to be resonantly enhanced in the  $\text{TR}^3$  spectra as well as some intensity in their overtones and combination bands. In some cases the even overtones of nontotally symmetric vibrational modes may also be present in the  $\text{TR}^3$  spectra. The  $\text{CH}_2\text{I}_2^+$  cation and  $\text{CH}_2\text{I}$  radical do not have two totally symmetric ( $A_1$ ) vibrational modes in the  $600\text{--}800$  region that are observed in the experimental  $\text{TR}^3$  spectra at  $720$  and  $600\text{ cm}^{-1}$  in the 0.5 M NaCl 75% water/25% acetonitrile solution and at  $701$  and  $619\text{ cm}^{-1}$  in the cyclohexane solvent. This suggests that the  $\text{CH}_2\text{I}_2^+$  cation and  $\text{CH}_2\text{I}$  radical species cannot account for the  $\text{TR}^3$  spectra in Figure S3 and Figure 5. The  $\text{CHI}$  carbene species has no predicted low-frequency mode (see Table S1) to correspond with the low-frequency mode ( $118$  to  $128\text{ cm}^{-1}$ ) seen in the  $\text{TR}^3$  spectra, which has significant overtones and combination bands with the two higher frequency fundamentals. This indicates the  $\text{CHI}$

carbene species cannot account for the  $\text{TR}^3$  spectra. The DFT predicted vibrational frequencies for the isodiiodomethane ( $\text{CH}_2\text{I}-\text{I}$ ) species are in reasonable agreement with the experimentally observed fundamentals of the  $\text{TR}^3$  spectra and can also account for the isotopic shifts in Raman vibrational frequencies when the parent molecule is fully deuterated (see Table S1 of the Supporting Information). Thus, the  $\text{TR}^3$  spectra appear to be due to the  $\text{CH}_2\text{I}-\text{I}$  species. Further support for this assignment comes from infrared spectra obtained after ultraviolet photolysis of  $\text{CH}_2\text{I}_2$  in low-temperature matrixes by Maier and co-workers.<sup>39,40</sup> These infrared spectra vibrational frequencies and their isotopic shifts in a fully deuterated compound are in good agreement with the DFT predicted vibrational frequencies for the  $\text{CH}_2\text{I}-\text{I}$  species (see Table S1). In particular, the infrared vibrational frequencies for the  $\nu_3$  C-I stretch ( $714/711\text{ cm}^{-1}$ ) and the  $\nu_4$   $\text{CH}_2$  wag ( $611\text{--}622\text{ cm}^{-1}$ ) modes are in good agreement with our  $\text{TR}^3$  Raman bands at  $701\text{--}720$  and  $600\text{--}619\text{ cm}^{-1}$ , respectively (see Table S1). The isotopic shifts for the fully deuterated species also display good agreement between the infrared and  $\text{TR}^3$  spectra in Table S1. Both the  $\text{TR}^3$  and infrared spectra vibrational frequencies can be reasonably assigned to the  $\text{CH}_2\text{I}-\text{I}$  species. The  $\text{TR}^3$  Raman band fundamentals are assigned as follows: the  $\nu_5$  (I-I stretch) mode to the Raman band near  $118\text{--}128\text{ cm}^{-1}$ , the  $\nu_4$  ( $\text{CH}_2$  wag) mode to the Raman band near  $600\text{--}620\text{ cm}^{-1}$ , and the  $\nu_3$  (C-I stretch) mode to the Raman band near  $701\text{--}720\text{ cm}^{-1}$  (see Table S1 as well). Similar assignments can be made for the  $\text{TR}^3$  spectra of isobromoiodomethane ( $\text{CH}_2\text{Br}-\text{I}$ ) and isochloroiodomethane ( $\text{CH}_2\text{Cl}-\text{I}$ ) and these assignments are given in Tables S2 and S3 in the Supporting Information, respectively.

The isodiiodomethane ( $\text{CH}_2\text{I}-\text{I}$ ) Raman band near  $715\text{ cm}^{-1}$  due to the nominal C-I stretch mode ( $\nu_3$ ), the isobromoiodomethane ( $\text{CH}_2\text{Br}-\text{I}$ ) Raman bands in the  $600\text{--}800\text{ cm}^{-1}$  region due to the fundamentals of the nominal C-Br stretch ( $\nu_3$ ) and  $\text{CH}_2$  wag ( $\nu_4$ ) vibrational modes, and the isochloroiodomethane ( $\text{CH}_2\text{Cl}-\text{I}$ ) Raman band near  $725\text{ cm}^{-1}$  due to the fundamental of the nominal C-Cl stretch vibrational mode were integrated at varying times to find the kinetics of the growth and decay of the isodihalomethane ( $\text{CH}_2\text{X}-\text{I}$ ) intermediates. Figure 6 shows plots of the relative integrated areas of the  $\nu_3$  Raman band of the  $\text{CH}_2\text{I}-\text{I}$  species from 0 to 500 ps, the  $\nu_3$  and  $\nu_4$  Raman bands of the  $\text{CH}_2\text{Br}-\text{I}$  species from 0 to 500 ps, and the  $\nu_4$  Raman band of the  $\text{CH}_2\text{Cl}-\text{I}$  species from 0 to 200 ps. In Figure 6 the open circles, stars, and squares represent data obtained in the 0.0 M NaCl, 0.2 M NaCl, and 0.5 M NaCl 75%  $\text{H}_2\text{O}/25\%$   $\text{CH}_3\text{CN}$  by volume solutions, respectively. These relative integrated areas of the relevant isodihalomethane Raman bands were fit to a simple function (denoted by the solid lines in Figure 6):

$$I(t) = Ae^{-t/t_1} - Be^{-t/t_2} \quad (2)$$

where  $I(t)$  is the relative integrated area of the relevant isodihalomethane Raman band,  $t$  is the time,  $t_1$  is the decay time constant of the Raman band,  $t_2$  is the growth time constant of the Raman band, and  $A$  and  $B$  are constants. The fits to the data in Figure 6 found decay time constants ( $t_1$ ) of 650, 480, and 430 ps for  $\text{CH}_2\text{I}-\text{I}$ , 130, 126, and 119 ps for  $\text{CH}_2\text{Br}-\text{I}$ , and 26, 26, and 27 ps for  $\text{CH}_2\text{Cl}-\text{I}$  in the 0.0, 0.2, and 0.5 M NaCl 75%  $\text{H}_2\text{O}/25\%$   $\text{CH}_3\text{CN}$  solutions, respectively. The lifetimes of the  $\text{CH}_2\text{X}-\text{I}$  (X = Cl, Br, I) species decrease as X changes from I to Br to Cl, which indicates the isodihalomethane intermediate becomes less stable as X becomes more electronegative. This is in agreement with the relative stability of isodihalomethanes in low-temperature matrixes where  $\text{CH}_2\text{I}-\text{I}$

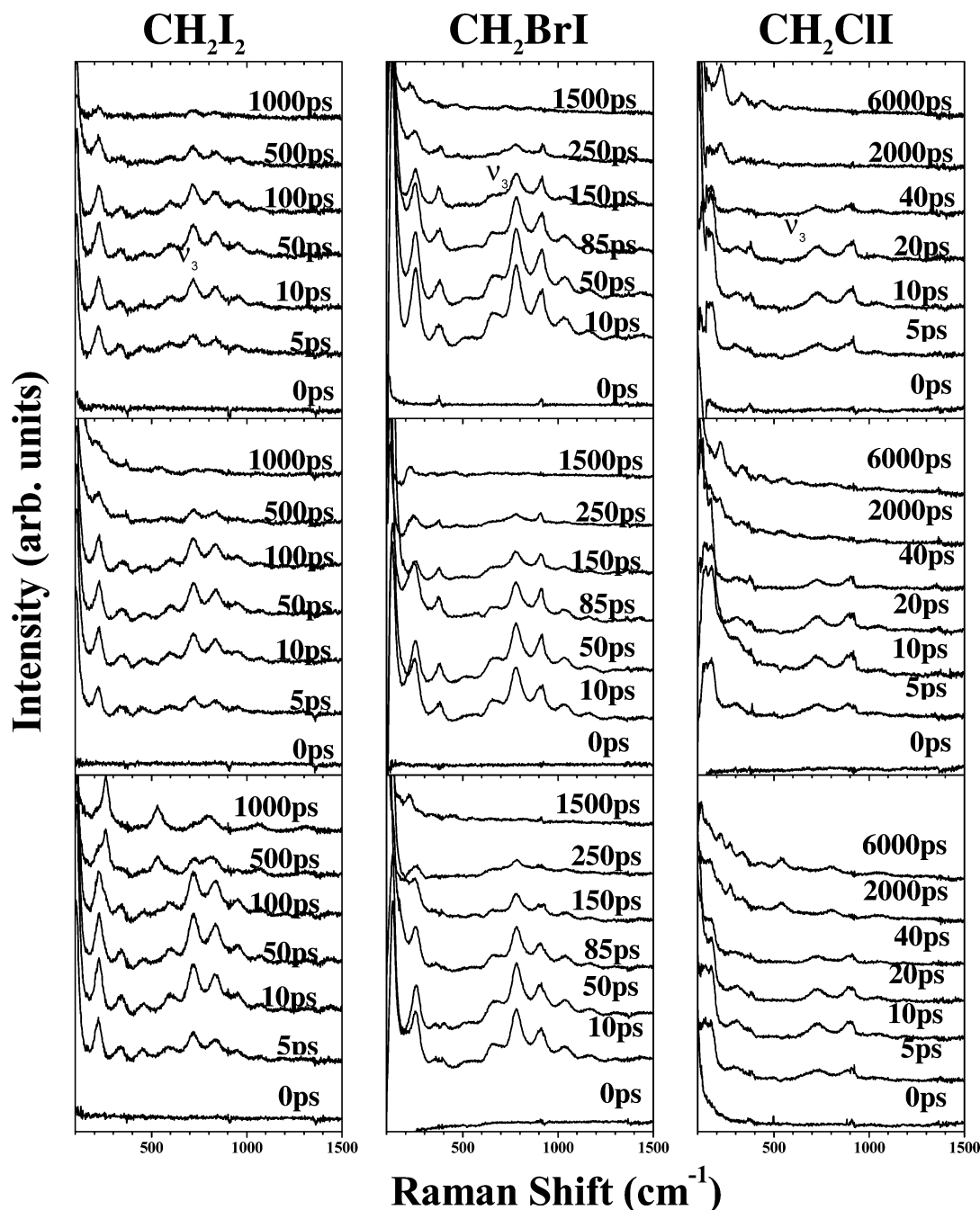


**Figure 5.** Stokes ps-TR<sup>3</sup> spectra (using a 400 nm probe wavelength) acquired after 267 nm photolysis of CH<sub>2</sub>I<sub>2</sub> (left column), CH<sub>2</sub>BrI (middle column), and CH<sub>2</sub>ClI (right column) in 0.0 M NaCl (top), 0.2 M NaCl (middle), and 0.5 M NaCl (bottom) 75% H<sub>2</sub>O/25% CH<sub>3</sub>CN solvents. Spectra were obtained at varying pump and probe time delays as indicated to the right of each spectrum. Assignments are indicated for some of the larger isodihalomethane Raman bands. See the text and refs 46, 47, 49, 52, 53, 55, and 58 for details of the assignments to the isodihalomethane species.

began to disappear at temperatures above 100 K whereas CH<sub>2</sub>-Cl-I began to disappear at temperatures around 26–30 K.<sup>39,40</sup> As the amount of salt in the solution increases, the decay of the CH<sub>2</sub>I-I species becomes moderately faster with a lifetime of about 650 ps in 0.0 M NaCl changing to about 430 ps in 0.5 M NaCl solution. However, the decay of the shorter lived CH<sub>2</sub>Br-I and CH<sub>2</sub>Cl-I species changes little if any as the salt concentration goes from 0.0 to 0.5 M NaCl. The lifetime of CH<sub>2</sub>Br-I goes from about 130 ps in 0.0 M NaCl to 119 ps in 0.5 M NaCl and the lifetime of CH<sub>2</sub>Cl-I remains about the same over the varying salt concentrations.

**Discussion of Photochemistry and Ps-TR<sup>3</sup> Results.** Examination of Figure 5 reveals that new prominent resonance Raman bands appear after photolysis of CH<sub>2</sub>I<sub>2</sub> at higher salt

concentrations (particularly at the 0.5 M NaCl concentration). These bands were found not to correlate with the decay of the isodiodomethane species and these new Raman bands were assigned to be due to the Cl<sub>2</sub><sup>-</sup> species.<sup>85</sup> This assignment was confirmed by comparison to authentic Cl<sub>2</sub><sup>-</sup> time-resolved resonance Raman spectra obtained from another reaction (photolysis of persulfate in the presence of Cl<sup>-</sup>)<sup>86</sup> and was described previously in ref 85. We note that formation of Cl<sub>2</sub><sup>-</sup> from several photochemistry reactions is known and has been characterized by time-resolved resonance Raman spectroscopy.<sup>86–88</sup> Inspection of the ps-TR<sup>3</sup> spectra in Figure 5 for the photolysis of CH<sub>2</sub>I<sub>2</sub> shows that as the salt concentration increases, the Cl<sub>2</sub><sup>-</sup> resonance Raman bands become more intense and have a faster appearance time. We proposed a possible

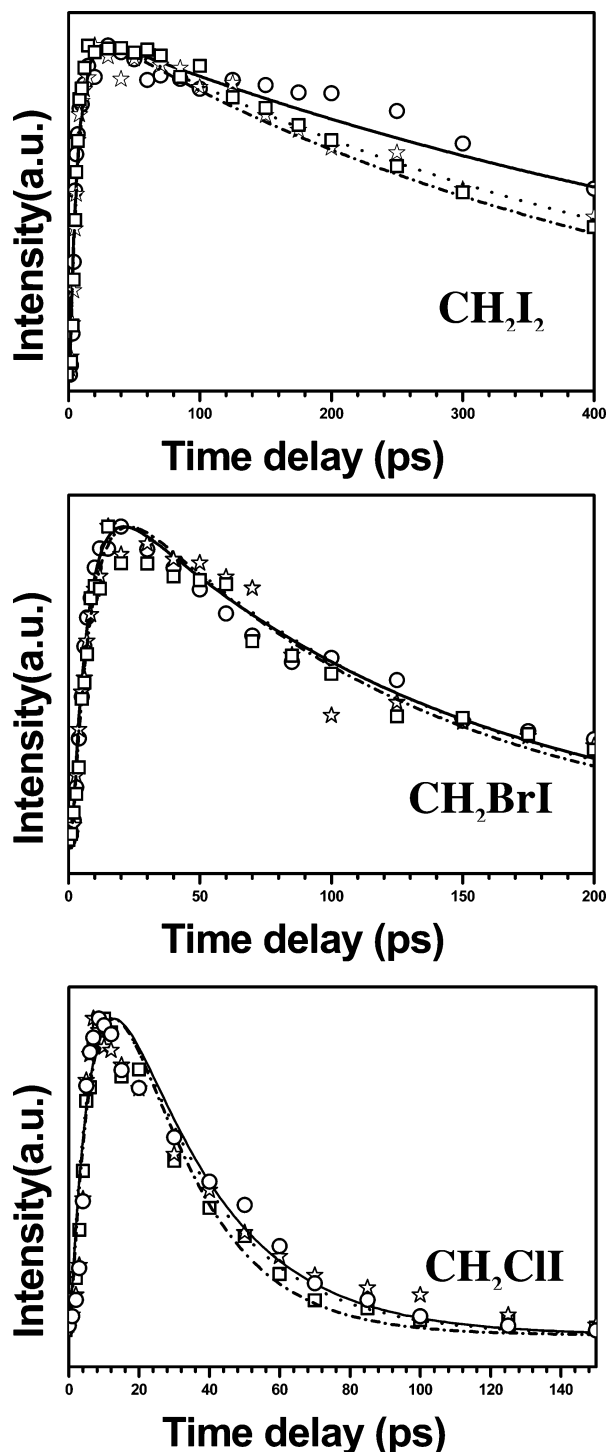
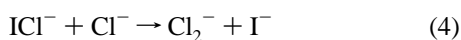


**Figure 6.** Plots of the relative integrated areas of the major isodihalomethane Raman bands ( $\nu_3$  Raman band for  $\text{CH}_2\text{I}-\text{I}$  (top),  $\nu_3$  and  $\nu_4$  Raman bands for  $\text{CH}_2\text{Br}-\text{I}$  (middle), and  $\nu_4$  Raman band for  $\text{CH}_2\text{Cl}-\text{I}$  (bottom)) at different delay times (from 0 to 6000 ps) obtained in 0.0 M NaCl (open circles), 0.02 M NaCl (open stars), and 0.5 M NaCl (open squares) 75%  $\text{H}_2\text{O}/25\%$   $\text{CH}_3\text{CN}$  solvents. The lines represent least-squares fits to the data (see the text for more details).

reaction mechanism for the fast formation of  $\text{Cl}_2^-$  after photolysis of  $\text{I}_2$  and  $\text{CH}_2\text{I}_2$  in saltwater (NaCl)/acetonitrile mixed solvents<sup>85</sup> and this is briefly described below:

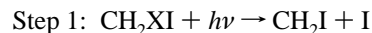


Reaction step 3 should occur very fast because the I atom can

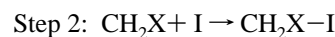
readily be scavenged by the high concentration of  $\text{Cl}^-$  in the solution and is forming a new  $\text{I}-\text{Cl}^-$  bond. Reaction step 4 can also be very fast since the  $\text{Cl}^-$  concentration is very high and it will produce a stronger bond ( $\text{Cl}_2^-$ ) than it is breaking ( $\text{I}-\text{Cl}^-$ ). We noted that photolysis of  $\text{I}_2$  or  $\text{CH}_2\text{I}_2$  in saltwater solutions did not form noticeable Raman bands of  $\text{ICl}^-$  at the 355 or 400 nm probe wavelengths employed in the TR<sup>3</sup> experiments. This may suggest that  $\text{ICl}^-$  is very short-lived and not a stable species in the presence of  $\text{Cl}^-$ . It may be possible that steps 3 and 4 both take place very fast and therefore do not lead to any concentration buildup of the  $\text{ICl}^-$  species so it would not be discernible in the TR<sup>3</sup> spectra.

We note that photolysis of  $\text{CH}_2\text{BrI}$  and  $\text{CH}_2\text{ClI}$  under the same conditions as  $\text{CH}_2\text{I}_2$  did not produce the same obvious  $\text{Cl}_2^-$  intermediate and this will be discussed further in a succeeding part of the discussion. Photolysis in saltwater solutions of all three dihalomethanes ( $\text{CH}_2\text{I}_2$ ,  $\text{CH}_2\text{BrI}$ , and  $\text{CH}_2\text{ClI}$ ) does produce noticeable amounts of the  $\text{CH}_2\text{XCl}$  ( $\text{X} = \text{I}, \text{Br}, \text{Cl}$ ) products respectively that were not found after photolysis in aqueous solutions without salt present. However, the major overall reaction present in both aqueous solutions without and with salt present is  $\text{CH}_2\text{XI} + h\nu \rightarrow \text{CH}_2(\text{OH})_2 + \text{HX} + \text{HI} + (n-2)\text{H}_2\text{O}$  in both cases. We have previously elucidated the following reaction mechanism for this reaction that we observe for ultraviolet photolysis of low concentrations of  $\text{CH}_2\text{XI}$  in aqueous solutions:

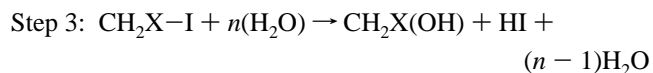
Photolysis of  $\text{CH}_2\text{XI}$  to form  $\text{CH}_2\text{X}$  and I fragments



Solvent-induced geminate recombination of the  $\text{CH}_2\text{X}$  and I fragments to form the  $\text{CH}_2\text{X}-\text{I}$  isomer



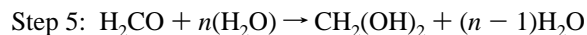
Water-catalyzed O-H insertion/HI elimination reaction of  $\text{CH}_2\text{X}-\text{I}$  with  $\text{H}_2\text{O}$  solvent



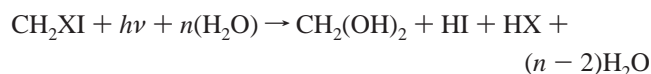
Water-catalyzed HX elimination reaction of  $\text{CH}_2\text{X}(\text{OH})$  with  $\text{H}_2\text{O}$  solvent



Water (and/or acid)-catalyzed addition of  $\text{H}_2\text{O}$  to  $\text{H}_2\text{CO}$  in  $\text{H}_2\text{O}$  solvent



Add steps 1–5 to obtain this overall reaction



The reader is referred to our previous work in refs 83–85 for more details about the preceding reaction mechanism.

In saltwater (NaCl) solutions different products ( $\text{CH}_2\text{XCl}$  where  $\text{X} = \text{I}, \text{Br}, \text{Cl}$ ) and a new intermediate  $\text{Cl}_2^-$  in the case of photolysis of  $\text{CH}_2\text{I}_2$  were seen that were not discernible in nonsalt aqueous solutions after photolysis of low concentrations of  $\text{CH}_2\text{XI}$  ( $\text{X} = \text{I}, \text{Br}, \text{Cl}$ ). This indicates these new products/intermediates are formed from some reaction(s) that involve NaCl. Our experiments indicate that the production of these new products/intermediates in saltwater solutions also lowers the relative amounts of  $\text{I}^-$  and  $\text{H}^+$  produced from each  $\text{CH}_2\text{XI}$  ( $\text{X} = \text{I}, \text{Br}, \text{Cl}$ ) molecule (see data in Figures 2 and 3). This suggests the amount of the highly reactive isodihalomethane ( $\text{CH}_2\text{X-I}$ ) species formed that then further reacts with water to eventually make the HI and HX leaving groups may be less in the presence of NaCl than in nonsalt aqueous environments. It is possible that reactions of NaCl with the initially produced  $\text{CH}_2\text{X}$  radical and I atom from the ultraviolet photolysis of the  $\text{CH}_2\text{XI}$  ( $\text{X} = \text{I}, \text{Br}, \text{Cl}$ ) molecules could possibly account for both a lower yield of the reactive isodihalomethane ( $\text{CH}_2\text{X-I}$ ) intermediates and the production of the different  $\text{CH}_2\text{XCl}$  ( $\text{X} = \text{I}, \text{Br}, \text{Cl}$ ) species observed in the saltwater photochemistry experiments. For instance, the reaction of the I atoms with  $\text{Cl}^-$  reaction to form the  $\text{ICl}^-$  species where it goes on to react with a  $\text{Cl}^-$  by reaction 4 to produce the  $\text{Cl}_2^-$  species can probably explain the formation of the  $\text{Cl}_2^-$  intermediate observed after photolysis of  $\text{CH}_2\text{I}_2$ . Similarly, the formation of the  $\text{CH}_2\text{XCl}$  ( $\text{X} = \text{I}, \text{Br}, \text{Cl}$ ) final products could probably be accounted for by one or more of the following reactions of the  $\text{CH}_2\text{X}$  radicals with species present in the reaction system:



We note that we were not able to directly follow the decay of the  $\text{CH}_2\text{X}$  radicals nor the formation of the  $\text{CH}_2\text{XCl}$  species since both types of species do not absorb appreciably at the probe wavelengths used in the  $\text{TR}^3$  experiments. Therefore, we could not determine the most likely reaction for the formation of the  $\text{CH}_2\text{XCl}$  final products. It is interesting to note that reaction 6 is similar to the  $\text{Cl}^\bullet + \text{Cl}_2^- \rightarrow \text{Cl}_2 + \text{Cl}^-$  reaction in aqueous solution recently investigated by Barker and co-workers.<sup>89</sup> In both reactions, a radical ( $\text{CH}_2\text{X}^\bullet$  or  $\text{Cl}^\bullet$ ) reacts with the  $\text{Cl}_2^-$  species to cleave its bond and form a new bond in the neutral species ( $\text{CH}_2\text{XCl}$  or  $\text{Cl}_2$ ) product and a halogen ion leaving group ( $\text{X}^-$  or  $\text{Cl}^-$ ). We also note that Moore and Zafiriou observed ultraviolet photolysis of seawater could lead to formation of noticeable amounts of  $\text{CH}_3\text{I}$  and they proposed this could be due to a fast  $\text{CH}_3 + \text{I}^- \rightarrow \text{CH}_3\text{I}$  reaction<sup>90</sup> that is similar to reaction 7 above. Thus, the similar radical reaction of  $\text{CH}_2\text{X} + \text{I}^-$  to form  $\text{CH}_2\text{XI}$  products may also occur in the saltwater solutions that we examine here. It is possible that the  $\text{CH}_2\text{XI}$  product observed after photolysis of the dihalomethanes in saltwater solutions could be formed from more than one type of reaction (for instance both reactions 6 and 7 above). Further work is needed to clarify the route(s) producing the  $\text{CH}_2\text{XI}$  products.

Why does the photolysis of low concentrations of  $\text{CH}_2\text{I}_2$  in saltwater lead to obvious resonance Raman bands for the  $\text{Cl}_2^-$  intermediate while the same experiments for  $\text{CH}_2\text{BrI}$  and  $\text{CH}_2\text{ClI}$  do not? The differences in the cage escape of the initially produced  $\text{CH}_2\text{X}$  and I photofragments and the relative chemical reactivity of the  $\text{CH}_2\text{X}$  radicals as X varies from I to Br and Cl in conjunction with the competition of reactions 5 and 6 can possibly explain this behavior. Femtosecond time-resolved transient absorption experiments by Åkesson, Sundström, Tarnovsky, and co-workers found that the quantum efficiency for the isomerization of  $\text{CH}_2\text{I}_2$  into  $\text{CH}_2\text{I-I}$  was about 70%,  $\text{CH}_2\text{BrI}$  into  $\text{CH}_2\text{Br-I}$  was about 26%, and  $\text{CH}_2\text{ClI}$  into  $\text{CH}_2\text{Cl-I}$  was about 9% after 266 nm photolysis in organic solvents.<sup>41–44</sup> Since the  $\text{CH}_2\text{X-I}$  isodihalomethanes are formed from solvent-induced geminate recombination of the initially produced fragments and the other fragments either undergo cage escape and/or form the parent  $\text{CH}_2\text{XI}$  molecules, this suggests that more cage escape of the initially formed photofragments occurs as one goes from photolysis of  $\text{CH}_2\text{I}_2$  to  $\text{CH}_2\text{BrI}$  and  $\text{CH}_2\text{ClI}$ . In addition, one could expect the chemical reactivity of the  $\text{CH}_2\text{X}$  radicals to increase significantly as one goes from  $\text{CH}_2\text{I}$  to  $\text{CH}_2\text{Br}$  and  $\text{CH}_2\text{Cl}$ . The photolysis of low concentrations of  $\text{CH}_2\text{I}_2$  in solution appears to lead to mostly formation of the highly reactive  $\text{CH}_2\text{I-I}$  isomer species and not much cage escape of the  $\text{CH}_2\text{I}$  radical photofragment. This and the lower reactivity of the  $\text{CH}_2\text{I}$  radical compared to the  $\text{CH}_2\text{Br}$  and  $\text{CH}_2\text{Cl}$  probably leads to reactions 5 and 6 to occur relatively slowly and allow a buildup of the  $\text{Cl}_2^-$  concentration that enables us to see the  $\text{Cl}_2^-$  species clearly in the ps- $\text{TR}^3$  experiments. However, 266 or 267 nm photolysis of  $\text{CH}_2\text{BrI}$  and  $\text{CH}_2\text{ClI}$  leads to much lower formation of their isodihalomethane species (26% and 9%, respectively) and this indicates there is likely significantly more cage escape of the  $\text{CH}_2\text{Br}$  and  $\text{CH}_2\text{Cl}$  radicals (especially considering these are smaller than the  $\text{CH}_2\text{I}$  radicals). This greater cage escape of these  $\text{CH}_2\text{X}$  ( $\text{X} = \text{Br}, \text{Cl}$ ) photofragments and their higher chemical reactivity compared to the  $\text{CH}_2\text{I}$  radicals probably leads to reactions 5 and 6 being very fast so that there is little noticeable buildup of the  $\text{Cl}_2^-$  intermediate and thus it is not easily observed in the ps- $\text{TR}^3$  experiments. Therefore, the differences in the yield for cage escape of the  $\text{CH}_2\text{X}$  photofragments and their relative chemical reactivity as X changes from I to Br and Cl can probably account for why the  $\text{Cl}_2^-$  intermediate can be readily observed after photolysis of  $\text{CH}_2\text{I}_2$  in saltwater while  $\text{Cl}_2^-$  is not easily observed after photolysis of  $\text{CH}_2\text{BrI}$  and  $\text{CH}_2\text{ClI}$  in saltwater. We note that in all three cases the final product produced will be the  $\text{CH}_2\text{XCl}$  ( $\text{X} = \text{I}, \text{Br}, \text{Cl}$ ) stable product observed in the NMR photochemistry experiments (see Figure 4).

**Discussion of Potential Implications for the Photochemistry of Dihalomethanes in Water and Saltwater Environments.** Ultraviolet photolysis of  $\text{CH}_2\text{XI}$  ( $\text{X} = \text{Cl}, \text{Br}, \text{I}$ ) at wavelengths longer than about 260 nm in the gas phase results in mainly direct C–I bond cleavage to form  $\text{CH}_2\text{X}$  radicals and I atom photofragments with a near unity quantum yield.<sup>22–29</sup> However, ultraviolet photolysis of low concentrations of  $\text{CH}_2\text{XI}$  ( $\text{X} = \text{Cl}, \text{Br}, \text{I}$ ) in aqueous environments without salt present was observed to result in mostly conversion of the parent molecule into  $\text{CH}_2(\text{OH})_2$  plus HI and HX products.<sup>83–85</sup> Similar photochemistry experiments for photolysis of  $\text{CH}_2\text{XI}$  in saltwater observed that the parent molecules are also mostly converted into  $\text{CH}_2(\text{OH})_2$  plus HI and HX products as well as noticeable amounts of  $\text{CH}_2\text{XCl}$  final products not observed in aqueous solutions without salt present. The preceding results demonstrate that the ultraviolet photochemistry of  $\text{CH}_2\text{XI}$  exhibits significant



phase dependence with very different reactions and products occurring in aqueous solutions compared to the gas phase. The reaction mechanism described in refs 83–85 (and very briefly here) can account for how the ultraviolet photolysis of  $\text{CH}_2\text{XI}$  at low concentrations in aqueous environments can lead to formation of  $\text{CH}_2(\text{OH})_2$  plus HI and HX products via some water-catalyzed dehalogenation reactions. These water-catalyzed dehalogenation reactions of isopolyhalomethanes and their reaction products could be noticeable sources of halogens and/or strong acids in the natural environment and this phase-dependent water-solvated photochemistry has yet to be considered in modeling the photochemistry of polyhalomethanes in the natural environment.

We performed several additional experiments using samples of  $\text{CH}_2\text{I}_2$  and  $\text{CH}_2\text{BrI}$  in water and 0.5 M NaCl water solutions that were housed in an airtight quartz tube and irradiated by natural sunlight (see Figures S4–S7 in the Supporting Information). Figure S4 shows absorption spectra acquired for  $1 \times 10^{-4}$  M solutions of  $\text{CH}_2\text{I}_2$  in water and 0.5 M NaCl saltwater after exposure to natural sunlight for 0, 2, 4, 6, 8, and 10 min. These spectra show that as  $\text{CH}_2\text{I}_2$  is photolyzed,  $\text{I}^-$  is produced and plots of  $-\Delta[\text{CH}_2\text{I}_2]$  versus  $[\text{I}^-]$  in Figure S4 indicate about 2  $\text{I}^-$  and 1.7  $\text{I}^-$  is produced from each  $\text{CH}_2\text{I}_2$  molecule following photolysis of  $\text{CH}_2\text{I}_2$  in water and saltwater, respectively. These results are very similar to the photolysis by laser experiments shown in Figures 1 and 2. Similar experiments were done with  $1.7 \times 10^{-4}$  M  $\text{CH}_2\text{I}_2$  in pure  $\text{D}_2\text{O}$  and 0.5 M NaCl salt  $\text{D}_2\text{O}$  and exposure to natural sunlight on a sunny day for about 30 min (from 12:10–12:40 pm).  $^1\text{H}$  NMR spectra were acquired before and after photolysis and are shown in Figure S5. The NMR spectra in Figure S5 show photolysis of  $\text{CH}_2\text{I}_2$  in pure  $\text{D}_2\text{O}$  leads to production of noticeable amounts of  $\text{CH}_2(\text{OD})_2$  while photolysis of  $\text{CH}_2\text{I}_2$  in the 0.5 M NaCl salt  $\text{D}_2\text{O}$  solution leads to production of appreciable amounts of both  $\text{CH}_2\text{ClI}$  and  $\text{CH}_2(\text{OD})_2$ . These results are similar to those found in the laser photochemistry experiments of Figure 4. Experiments with  $2 \times 10^{-4}$  M  $\text{CH}_2\text{BrI}$  in pure water and in 0.5 M NaCl saltwater and exposure to natural sunlight for 0, 15, 45, 85, and 125 min are presented in Figure S6 and show production of  $\text{I}^-$  after photolysis of  $\text{CH}_2\text{BrI}$  similar to results from laser photolysis experiments shown in Figure 1. Similar experiments were done with  $2.0 \times 10^{-4}$  M  $\text{CH}_2\text{BrI}$  in pure  $\text{D}_2\text{O}$  and 0.5 M NaCl salt  $\text{D}_2\text{O}$  and exposure to natural sunlight on a sunny day for about 150 min (from 13:10–15:40 pm).  $^1\text{H}$  NMR spectra were acquired before and after photolysis and are shown in Figure S7. The NMR spectra in Figure S7 show photolysis of  $\text{CH}_2\text{BrI}$  in pure  $\text{D}_2\text{O}$  leads to production of noticeable amounts of  $\text{CH}_2(\text{OD})_2$  while photolysis of  $\text{CH}_2\text{BrI}$  in the 0.5 M NaCl salt  $\text{D}_2\text{O}$  solution leads to formation of appreciable amounts of both  $\text{CH}_2\text{BrCl}$  and  $\text{CH}_2(\text{OD})_2$ . These results are similar to those found in the laser photochemistry experiments of Figure 4. The preceding results for  $\text{CH}_2\text{I}_2$  and  $\text{CH}_2\text{BrI}$  indicate photolysis of relatively low concentrations in water and saltwater solutions by natural sunlight (see Figures S4–S7 of the Supporting Information) leads to results very similar to those using laser photolysis (see Figures 1, 2, and 4). Since the 0.5 M NaCl solutions have salt concentrations similar to the salt concentration of seawater, the preceding results for the natural light photolysis of  $\text{CH}_2\text{I}_2$  and  $\text{CH}_2\text{BrI}$  in the saltwater solutions suggest that similar photochemistry may also occur in seawater in the natural environment.

We note that  $\text{CH}_2\text{I}_2$ ,  $\text{CH}_2\text{BrI}$ , and  $\text{CH}_2\text{ClI}$  and other polyhalomethanes have been observed in seawater and in the marine boundary layer of the troposphere and their presence attributed

mainly to biogenic sources such as seaweed and/or microalgae.<sup>7,91,92</sup> It is interesting that the measured seawater levels of  $\text{CH}_2\text{I}_2$  and  $\text{CH}_2\text{IBr}$  were determined to be lower than those computed from seaweed production and this is probably due to photodissociation in the water column.<sup>91,92</sup> However, the amounts of  $\text{CH}_3\text{I}$  and  $\text{CH}_2\text{ClI}$  computed from the emission rates and biomass estimates could not account for the high level of these species in surface coastal waters. This could be due to additional marine sources of these compounds. Our present work has found that photolysis of low concentrations of  $\text{CH}_2\text{XI}$  in saltwater (with NaCl concentrations similar to those of seawater) leads to production of some  $\text{CH}_2\text{XCl}$  products not observed in aqueous solutions without salt present. We note that this could be a new photochemical route or marine source of  $\text{CH}_2\text{XCl}$  species such as  $\text{CH}_2\text{ICl}$  that could possibly help explain the higher than expected amounts of  $\text{CH}_2\text{ICl}$  observed in coastal waters. The relatively strong absorption of  $\text{CH}_2\text{I}_2$  above 300 nm in the sunlight region results in it having a very short lifetime in the natural environment due to its quick photodissociation. However,  $\text{CH}_2\text{ICl}$  and other  $\text{CH}_2\text{XCl}$  molecules have little absorption in the sunlight region and would have substantially longer lifetimes in the natural environment in the marine boundary layer. This indicates that  $\text{CH}_2\text{ICl}$  produced from the photolysis of  $\text{CH}_2\text{I}_2$  in seawater could still be noticeable long after the precursor  $\text{CH}_2\text{I}_2$  disappears. It would be interesting to investigate whether the photolysis of  $\text{CH}_2\text{I}_2$  and  $\text{CH}_2\text{BrI}$  in coastal waters is correlated to the formation of some additional  $\text{CH}_2\text{ICl}$  and  $\text{CH}_2\text{BrCl}$ , respectively, in coastal waters. The production of  $\text{CH}_2\text{XCl}$  species such as  $\text{CH}_2\text{ICl}$  and  $\text{CH}_2\text{BrCl}$  could possibly also be utilized as a marker or indicator for the photolysis of  $\text{CH}_2\text{XI}$  species in saltwater environments compared to water solvated environments without salt present.

Our present work and comparison of the photochemistry of  $\text{CH}_2\text{XI}$  ( $\text{X} = \text{Cl}, \text{Br}, \text{I}$ ) nonsalt and salt aqueous solutions may also have some interesting implications for the photolysis of polyhalomethanes in aqueous sea-salt particles. At fairly low concentrations to moderate concentrations of NaCl comparable to that in seawater, there will still be significant formation of isopolyhalomethanes and their associated reactions with water to release strong acids (HX). Employing  $\text{CH}_2\text{I}_2$  as an example, the HI strong acid and methanediol products formed from the photolysis of  $\text{CH}_2\text{I}_2$  will be accompanied by some production of  $\text{CH}_2\text{ICl}$ . As the salt concentration increases further, one could expect that the production of strong acids via the water-catalyzed reactions would decrease with more products produced from the reactions of the initially formed  $\text{CH}_2\text{X}$  and I photofragments. Thus, the production of strong acids and potential halogen activation may vary strongly with the level of water or salt in the aqueous sea-salt particles. A great deal more study is needed to better understand the photochemistry of polyhalomethanes in a range of water-solvated environments present in the natural environment.

## Conclusions

A series of dihalomethanes ( $\text{CH}_2\text{I}_2$ ,  $\text{CH}_2\text{BrI}$ , and  $\text{CH}_2\text{ClI}$ ) were photolyzed in saltwater environments and compared to results recently obtained in aqueous environments where salt is absent. These photochemistry experiments found that ultraviolet photolysis of low concentrations of all three  $\text{CH}_2\text{XI}$  molecules in saltwater resulted in mostly formation of  $\text{CH}_2(\text{OH})_2$  and HX and HI products similar to photolysis in aqueous solvents with no salt present. However, new  $\text{CH}_2\text{XCl}$  (where  $\text{X} = \text{Cl}, \text{Br}, \text{I}$ ) products were formed to a noticeable degree in the saltwater solvents. These new  $\text{CH}_2\text{XCl}$  products

did not appear after photolysis of the  $\text{CH}_2\text{XI}$  molecules in aqueous solutions without salt present. We briefly discussed possible mechanism(s) for the formation of these  $\text{CH}_2\text{XCl}$  products in saltwater solutions. We also very briefly discussed the potential influence of this photochemistry on the degradation of polyhalomethanes in aqueous environments with and without salt present.

**Acknowledgment.** This work was supported by grants from the Research Grants Council (RGC) of Hong Kong (HKU 7036/04P and HKU 1/01C) to D.L.P. W.M.K. thanks the University of Hong Kong for the award of a Research Assistant Professorship.

**Supporting Information Available:** Absorption spectra of different concentrations of  $\text{CH}_2\text{I}_2$  dissolved in water and a plot of the absorption versus  $\text{CH}_2\text{I}_2$  concentration from the absorption spectra data (Figure S1); absorption spectra of different concentrations of NaI dissolved in water and a plot of the absorption of  $\text{I}^-$  versus NaI concentration from the absorption data (Figure S2); comparison of  $\text{TR}^3$  spectra (Figure S3) of isodiodomethane obtained in cyclohexane solvent using a nanosecond pulsed laser, in cyclohexane solvent at 500 ps using a picosecond laser (from ref 50), in acetonitrile solvent at 100 ps using a picosecond laser (from ref 50) and in a 0.5 M NaCl 75% water/25% acetonitrile solution using a picosecond laser (this work); absorption spectra of  $\text{CH}_2\text{I}_2$  in pure water and in 0.5 M NaCl saltwater under natural sunlight irradiation and the plots of  $-\text{[CH}_2\text{I}_2]$  versus  $[\text{I}^-]$  for photolysis of  $\text{CH}_2\text{I}_2$  in water and 0.5 M NaCl solution (Figure S4);  $^1\text{H}$  NMR spectra obtained for  $\text{CH}_2\text{I}_2$  in pure  $\text{D}_2\text{O}$  and in 0.5 M NaCl salt  $\text{D}_2\text{O}$  before and after natural sunlight irradiation (Figure S5); absorption spectra of  $\text{CH}_2\text{BrI}$  in pure water and in 0.5 M NaCl saltwater under natural sunlight irradiation (Figure S6);  $^1\text{H}$  NMR spectra obtained for  $\text{CH}_2\text{BrI}$  in pure  $\text{D}_2\text{O}$  and in 0.5 M NaCl salt  $\text{D}_2\text{O}$  before and after natural sunlight irradiation (Figure S7); vibrational assignments for the present isopolyhalomethane spectra and comparison to previous vibrational assignments as well as to previously predicted vibrational frequencies for the relevant isodihalomethanes and several other species that have been proposed to be formed after photolysis of dihalomethanes in condensed phase environments (Tables S1–S3). This material is available free of charge via the Internet at <http://pubs.acs.org>.

## References and Notes

- Class, Th.; Ballschmiter, K. *J. Atmos. Chem.* **1988**, *6*, 35–46.
- Klick, S.; Abrahamsson, K. *J. Geophys. Res.* **1992**, *97*, 12683–12687.
- Heumann, K. G. *Anal. Chim. Acta* **1993**, *283*, 230–245.
- Moore, R. M.; Webb, M.; Tokarczyk, R.; Wever, R. *J. Geophys. Res.-Oceans* **1996**, *101*, No. C9, 20899–20908.
- McElroy, C. T.; McLinden, C. A.; McConnell, J. C. *Nature* **1997**, *397*, 338–341.
- Mössigner, J. C.; Shallcross, D. E.; Cox, R. A. *J. Chem. Soc., Faraday Trans.* **1998**, *94*, 1391–1396.
- Carpenter, L. J.; Sturges, W. T.; Penkett, S. A.; Liss, P. S. *J. Geophys. Res.-Atmos* **1999**, *104*, 1679–1689.
- Alicke, B.; Hebstreit, K.; Stutz, J.; Platt, U. *Nature* **1999**, *397*, 572–573.
- O'Dowd, C. D.; Jimenez, J. L.; Bahreini, R.; Pagan, R. C.; Seinfeld, J. H.; Hamerl, K.; Pirjola, L.; Kulmala, M.; Jennings, S. G.; Hoffmann, T. *Nature* **2002**, *417*, 632–636.
- Wayne, R. P. *Chemistry of Atmospheres*, 3rd ed.; Oxford University Press: Oxford, U.K., 2000.
- Fan, S. F.; Jacob, D. J. *Nature* **1992**, *359*, 522–524.
- Mozurkewich, M. *J. Geophys. Res.* **1995**, *100*, D7, 14199–14207.
- Vogt, R.; Crutzen, P. J.; Sander, S. *Nature* **1996**, *383*, 327–330.
- Sander, R.; Crutzen, P. J. *J. Geophys. Res.* **1996**, *101*, D4, 9121–9138.
- Oum, K. W.; Lakin, M. J.; DeHaan, D. O.; Brauers, T.; Finalyson-Pitts, B. J. *Science* **1998**, *279*, 74–77.
- McElroy, C. T.; McLinden, C. A.; McConnell, J. C. *Nature* **1999**, *397*, 338–341.
- Vogt, R.; Sander, R.; Glasow, R. V.; Crutzen, P. J. *J. Atmos. Chem.* **1999**, *32*, 375–395.
- Behnke, W.; Elend, M.; Krüger, U.; Zetzsch, C. *J. Atmos. Chem.* **1999**, *34*, 87–99.
- Knipping, E. M.; Lakin, M. J.; Foster, K. L.; Jungwirth, P.; Tobias, D. J.; Gerber, R. B.; Dabdub, D.; Finalyson-Pitts, B. J. *Science* **2000**, *288*, 301–306.
- Finalyson-Pitts, B. J.; Hemminger, J. C. *J. Phys. Chem. A* **2000**, *104*, 11463–11477.
- Foster, K. L.; Plastring, R. A.; Bottenheim, J. W.; Shepson, P. B.; Finalyson-Pitts, B. J.; Spicer, C. W. *Science* **2001**, *291*, 471–474.
- Kawasaki, M.; Lee, S. J.; Bersohn, R. *J. Chem. Phys.* **1975**, *63*, 809–814.
- Schmitt, G.; Comes, F. J. *J. Photochem.* **1980**, *14*, 107–123.
- Kroger, P. M.; Demou, P. C.; Riley, S. J. *J. Chem. Phys.* **1976**, *65*, 1823–1834.
- Koffend, J. B.; Leone, S. R. *Chem. Phys. Lett.* **1981**, *81*, 136–141.
- Cain, S. R.; Hoffman, R.; Grant, R. *J. Phys. Chem.* **1981**, *85*, 4046–4051.
- Lee, S. J.; Bersohn, R. *J. Phys. Chem.* **1982**, *86*, 728–730.
- Butler, L. J.; Hints, E. J.; Lee, Y. T. *J. Chem. Phys.* **1986**, *84*, 4104–4106.
- Butler, L. J.; Hints, E. J.; Lee, Y. T. *J. Chem. Phys.* **1987**, *86*, 2051–2074.
- Wannenmacher, E. A. J.; Felder, P.; Huber, J. R. *J. Chem. Phys.* **1991**, *95*, 986–997.
- Baum, G.; Felder, P.; Huber, J. R. *J. Chem. Phys.* **1993**, *98*, 1999–2010.
- Marvet, U.; Dantus, M. *Chem. Phys. Lett.* **1996**, *256*, 57–62.
- Zhang, Q.; Marvet, U.; Dantus, M. *J. Chem. Phys.* **1998**, *109*, 4428–4442.
- Jung, K.-W.; Ahmadi, T. S.; El-Sayed, M. A. *Bull. Korean Chem. Soc.* **1997**, *18*, 1274–1280.
- Radloff, W.; Farmanara, P.; Stert, V.; Schreiber, E.; Huber, J. R. *Chem. Phys. Lett.* **1998**, *291*, 173–178.
- Kavita, K.; Das, P. K. *J. Chem. Phys.* **2000**, *112*, 8426–8431.
- Baughcum, S. L.; Hafmann, H.; Leone, S. R.; Nesbitt, D. *Faraday Discuss.* **1979**, *67*, 306–315.
- Baughcum, S. L.; Leone, S. R. *J. Chem. Phys.* **1980**, *72*, 6531–6545.
- Maier, G.; Reisenauer, H. P. *Angew. Chem., Int. Ed. Engl.* **1986**, *25*, 819–822.
- Maier, G.; Reisenauer, H. P.; Lu, J.; Schaad, L. J.; Hess, B. A., Jr. *J. Am. Chem. Soc.* **1990**, *112*, 5117–5122.
- Tarnovsky, A. N.; Alvarez, J.-L.; Yartsev, A. P.; Sündstrom, V.; Åkesson, E. *Chem. Phys. Lett.* **1999**, *312*, 121–130.
- Tarnovsky, A. N.; Wall, M.; Rasmusson, M.; Pascher, T.; Åkesson, E. *J. Chin. Chem. Soc.* **2000**, *47*, 769–772.
- Tarnovsky, A. N.; Wall, M.; Gustafsson, M.; Lascoux, N.; Sundström, V.; Åkesson, E. *J. Phys. Chem. A* **2002**, *106*, 5999–6005.
- Wall, M.; Tarnovsky, A. N.; Pascher, T.; Sundström, V.; Åkesson, E. *J. Phys. Chem. A* **2003**, *107*, 211–217.
- Zheng, X.; Phillips, D. L. *Chem. Phys. Lett.* **2000**, *324*, 175–182.
- Zheng, X.; Phillips, D. L. *J. Chem. Phys.* **2000**, *113*, 3194–3203.
- Zheng, X.; Phillips, D. L. *J. Phys. Chem. A* **2000**, *104*, 6880–6886.
- Zheng, X.; Kwok, W. M.; Phillips, D. L. *J. Phys. Chem. A* **2000**, *104*, 10464–10470.
- Zheng, X.; Fang, W.-H.; Phillips, D. L. *J. Chem. Phys.* **2000**, *113*, 10934–10946.
- Kwok, W. M.; Ma, C.; Parker, A. W.; Phillips, D.; Towrie, M.; Matousek, P.; Phillips, D. L. *J. Chem. Phys.* **2000**, *113*, 7471–7478.
- Zheng, X.; Lee, C. W.; Li, Y.-L.; Fang, W.-H.; Phillips, D. L. *J. Chem. Phys.* **2001**, *114*, 8347–8356.
- Kwok, W. M.; Ma, C.; Parker, A. W.; Phillips, D.; Towrie, M.; Matousek, P.; Zheng, X.; Phillips, D. L. *J. Chem. Phys.* **2001**, *114*, 7536–7543.
- Kwok, W. M.; Ma, C.; Parker, A. W.; Phillips, D.; Towrie, M.; Matousek, P.; Phillips, D. L. *Chem. Phys. Lett.* **2001**, *341*, 292–298.
- Li, Y.-L.; Wang, D.; Phillips, D. L. *Bull. Chem. Soc. Jpn.* **2002**, *75*, 943–948.
- Kwok, W. M.; Ma, C.; Parker, A. W.; Phillips, D.; Towrie, M.; Matousek, P.; Phillips, D. L. *J. Phys. Chem. A* **2003**, *107*, 2624–2628.
- Andrews, L.; Prochaska, F. T.; Ault, B. S. *J. Am. Chem. Soc.* **1979**, *101*, 9–15.
- Mohan, H.; Iyer, R. M. *Radiat. Eff.* **1978**, *39*, 97–101.
- Mohan, H.; Moorthy, P. N. *J. Chem. Soc., Perkin Trans. 2* **1990**, 277–282.

- (59) Schwartz, B. J.; King, J. C.; Zhang, J. Z.; Harris, C. B. *Chem. Phys. Lett.* **1993**, 203, 503–508.
- (60) Saitow, K.; Naitoh, Y.; Tominaga, K.; Yoshihara, K. *Chem. Phys. Lett.* **1996**, 262, 621–626.
- (61) Kropp, P. J.; Pienta, N. J.; Sawyer, J. A.; Polniaszek, R. P. *Tetrahedron* **1981**, 37, 3229–3236.
- (62) Kropp, P. J. *Acc. Chem. Res.* **1984**, 17, 131–137.
- (63) Phillips, D. L.; Fang, W.-H.; Zheng, X. *J. Am. Chem. Soc.* **2001**, 123, 4197–4203.
- (64) Phillips, D. L.; Fang, W.-H. *J. Org. Chem.* **2001**, 66, 5890–5896.
- (65) Li, Y.-L.; Leung, K. H.; Phillips, D. L. *J. Phys. Chem. A* **2001**, 105, 10621–10625.
- (66) Fang, W.-H.; Phillips, D. L.; Wang, D.; Li, Y.-L. *J. Org. Chem.* **2002**, 67, 154–160.
- (67) Li, Y.-L.; Chen, D. M.; Wang, D.; Phillips, D. L. *J. Org. Chem.* **2002**, 67, 4228–4235.
- (68) Li, Y.-L.; Wang, D.; Phillips, D. L. *J. Chem. Phys.* **2002**, 117, 7931–7941.
- (69) Phillips, D. L.; Fang, W.-H.; Zheng, X.; Li, Y.-L.; Wang, D.; Kwok, W. M. *Curr. Org. Chem.* **2004**, 8, 739–755.
- (70) Tarnovsky, A. N.; Sundstrom, V.; Akesson, E.; Pascher, T. *J. Phys. Chem. A* **2004**, 108, 237–249.
- (71) Harding, L. B.; Schlegel, H. B.; Krishnan, R.; Pople, J. A. *J. Phys. Chem.* **1980**, 84, 3394–3401.
- (72) Pople, J. A.; Raghavachari, K.; Frisch, M. J.; Binkley, J. B.; Schleyer, P. v. R. *J. Am. Chem. Soc.* **1983**, 105, 6389–6398.
- (73) Wesdemiotis, C.; Feng, R.; Danis, P. O.; Williams, E. R.; Lafferty, F. W. *J. Am. Chem. Soc.* **1986**, 108, 5847–5853.
- (74) Yates, B. F.; Bouma, W. J.; Radom, L. *J. Am. Chem. Soc.* **1987**, 109, 2250–2263.
- (75) Kirmse, W.; Meinert, T.; Moderelli, D. A.; Platz, M. S. *J. Am. Chem. Soc.* **1993**, 115, 8918–8927.
- (76) Walch, S. P. *J. Chem. Phys.* **1993**, 98, 3163–3178.
- (77) Gonzalez, C.; Restrepo-Cossio, A.; Márquez, M.; Wiberg, K. B. *J. Am. Chem. Soc.* **1996**, 118, 5408–5411.
- (78) Moody, C. J.; Whitman, G. H. In *Reactive Intermediates*; Davies, S. G., Ed.; Oxford University Press: New York, 1992.
- (79) Pliego, J. R., Jr.; De Almeida, W. B. *J. Phys. Chem.* **1996**, 100, 12410–12413.
- (80) Pliego, J. R., Jr.; De Almeida, W. B. *J. Phys. Chem. A* **1999**, 103, 3904–3909.
- (81) Kwok, W. M.; Zhao, C.; Li, Y. L.; Guan, X.; Phillips, D. L. *J. Chem. Phys.* **2004**, 120, 3323–3332.
- (82) Kwok, W. M.; Zhao, C.; Li, Y. L.; Guan, X.; Wang, D.; Phillips, D. L. *J. Am. Chem. Soc.* **2004**, 126, 3119–3131.
- (83) Kwok, W. M.; Zhao, C.; Guan, X.; Li, Y. L.; Du, Y.; Phillips, D. L. *J. Chem. Phys.* **2004**, 120, 9017–9032.
- (84) Lin, X.; Guan, X.; Kwok, W. M.; Zhao, C.; Du, Y.; Li, Y.-L.; Phillips, D. L. *J. Phys. Chem. A* **2005**, 109, 981–998.
- (85) Guan, X.; Du, Y.; Li, Y.-L.; Kwok, W. M.; Phillips, D. L. *J. Chem. Phys.* **2004**, 121, 8399–8409.
- (86) Hynes, A. J.; Wine, P. H. *J. Chem. Phys.* **1988**, 89, 3565–3572.
- (87) Wilbrandt, R.; Jensen, N. H.; Silensen, A. H.; Hansen, K. B. *Chem. Phys. Lett.* **1984**, 106, 503–507.
- (88) Tripathi, G. N. R.; Schuler, R. H.; Fessenden, R. W. *Chem. Phys. Lett.* **1985**, 113, 563–568.
- (89) Yu, X.-Y.; Bao, Z.-C.; Barker, J. R. *J. Phys. Chem. A* **2004**, 108, 295–308.
- (90) Moore, R. M.; Zafiriou, O. C. *J. Geophys. Res.* **1994**, 99, 16415–16420.
- (91) Carpenter, L. J.; Malin, G.; Kuepper, F.; Liss, P. S. *Global Biogeochem. Cycles* **2000**, 14, 1191–1204.
- (92) Carpenter, L. J. *Chem. Rev.* **2003**, 103, 4953–4962.